European Journal of Chemistry

View Journal Online
View Article Online

A new polymorph of 5-bromo ortho vanillin: Synthesis, characterization, crystal engineering, Hirshfeld surface, calculation of interaction energy, and energy frameworks

Sourav Roy [1], Dhrubajyoti Majumdar [2,*] and Dhiraj Das [3]

[1] *Solid State and Structural Chemistry Unit, Indian Institute of Science, Bangalore 560 012, India*
[2] *Department of Chemistry, Tamralipta Mahavidyalaya, Tamluk-721636, West Bengal, India*
[3] *Basic Science and Humanities, Indian Naval Academy, Ezhimala, Kannur-670310, Kerala, India*

* *Corresponding author at: Department of Chemistry, Tamralipta Mahavidyalaya, Tamluk-721636, West Bengal, India.*
e-mail: dmajumdar@tmv.ac.in (Dhrubajyoti Majumdar).

RESEARCH ARTICLE

10.5155/eurjchem.17.2.168-175.2796

Received: 5 April 2026
Received in revised form: 5 May 2026
Accepted: 15 May 2026
Published online: 30 June 2026
Printed: 30 June 2026

KEYWORDS

Polymorph
Crystal structure
Hirshfeld surface
Energy frameworks
5-Bromo ortho vanillin
Energy interaction energy

ABSTRACT

This article reports on one of the newly synthesized 5-bromo ortho vanillin ($C_8H_7BrO_3$) (1) polymorphs, whose X-ray structure was determined by single crystal X-ray diffraction. The polymorph attains a monoclinic system, space group $P2_1/c$, V = 824.3(9), and Z = 4. In this work, the cell parameters observed are a = 4.080(2) Å, b = 20.733(12) Å, c = 9.844(7) Å, and β = 98.4(2). Polymorph 1 is compared with the reported compound 2. The article discusses the structural characterization of polymorph 1 using HRMS, FTIR, UV-vis, $^1H/^{13}C$ NMR, and ^{13}C DEPT NMR spectroscopy, and explores NCSI (noncovalent supramolecular interactions) within the crystal network. Furthermore, the Hirshfeld surface and 2D fingerprint plot analyze the presence of significant H···Br (20.8%) and H···O (23.8%) contacts in the crystal assembly. In addition, interaction energies and energy frameworks have been calculated. The study revealed that the constructed frameworks fall into electrostatic (E_{ele}, red cylinders) and dispersion (E_{dis}, green cylinders) categories, along with total interaction energies (E_{tot}, blue cylinders). The polymorph is rationalized using physicochemical, crystallographic, Hirshfeld surface, interaction energy and energy frameworks.

Cite this: *Eur. J. Chem.* **2026**, *17(2)*, 168-175 **Journal website**: www.eurjchem.com

1. Introduction

In recent years, crystal engineering concepts of Br polymorphs have been used to exploit noncovalent interactions (NCI), such as hydrogen bonding, and this approach ultimately designs crystal packing [1]. Hence, the chemistry of polymorphs and crystal engineering are closely linked to each other. In 1955, Pepinsky and Schmidt first revealed the concept of crystal engineering [2]. The concept of the current phase was further formulated by G. Desiraju in 1989, following the publication of his own book [3]. Subsequently, the crystal engineering approach controls the overall crystallization process and chemically identifies polymorphs [1]. Polymorphs are distinct crystalline forms of the same molecule, but each has distinct physical properties, including solubility, stability, and melting point. The term polymorphs refers to the ability of a molecule to exist in more than one crystalline state [1,4-6]. The differences in polymorph properties would arise from differences in molecular stacking or conformation [7]. In crystal engineering, several processes accelerate the formation of polymorphs. Key techniques include solution crystallization, solvent variation, and control of the cooling rate [1,8,9]. The polymorphs synthesized under this experimental environment are stable or metastable, from a free-energy perspective [10-12]. The latter variety has a high free energy and enhanced solubility and has gained importance in drug chemistry. In this context, it is worth noting that a crystal engineering strategy has emerged to improve the solubility of polymorphs [11,12]. Again, over the past decade, the concept of polymorphic drug research has been widely used in crystal structure prediction. Moreover, in recent years, Br (brominated) organic polymorphs have attracted a great deal of research attention, especially for organic synthetic chemists [1]. These classified polymorphs exhibited variable physical properties, including solubility, melting point, and color. They are also exploring C-H···O or N-O···Br supramolecular interactions in their crystal networks [13-16]. In particular, these research areas have several examples documented in the literature, such as picryl bromide [16,17], 4-bromo-2,7-di-*tert*-butyl-9-methoxypyrene [16], 2-(5-bromo-4-(4-cyclopropylnaphthalen-1-yl)-4*H*-1,2,4-triazol-3-ylthio) acetic acid, 1-bromo-3,5,7-trimethyladamantane [18] and 4-bromo-2-[(phenylimino)methyl]phenol [19]. Moreover, there are several interesting features of Br polymorphs.

https://dx.doi.org/10.5155/eurjchem.17.2.168-175.2796

Table 1. Polymorph crystal data and structure refinement parameters.

Identification code	1 (Polymorph)	2 (Reported compound)
Empirical formula	$C_8H_7BrO_3$	$C_8H_7BrO_3$
Formula weight (g/mol)	231.05	231.05
Temperature (K)	100(2)	296(2)
Crystal system	Monoclinic	Monoclinic
Space group	$P2_1/c$	$P2_1/c$
a (Å)	4.080(2)	13.154(3)
b (Å)	20.733(12)	9.4175(18)
c (Å)	9.844(7)	6.9853(14)
β (°)	98.14(2)	103.834(5)
Volume (Å^3)	824.3(9)	840.2(3)
Z	4	4
ρ_{calc} (g/cm^3)	1.862	1.827
μ (mm^{-1})	4.946	4.853
F(000)	456.0	456.0
Crystal size (mm^3)	0.18 × 0.12 × 0.08	0.23 × 0.12 × 0.08
Radiation	MoKα (λ = 0.71073)	MoKα (λ = 0.71073)
2Θ range for data collection (°)	3.93 to 50.19	3.188 to 50.118
Index ranges	$-4 \le h \le 4$, $-24 \le k \le 24$, $-11 \le l \le 11$	$-15 \le h \le 15$, $-11 \le k \le 11$, $-8 \le l \le 8$
Reflections collected	22160	25414
Independent reflections	1437 [R_{int} = 0.0564, R_{sigma} = 0.0239]	1474 [R_{int} = 0.1011, R_{sigma} = 0.0419]
Data/restraints/parameters	1437/0/111	1474/0/112
Goodness-of-fit on F^2	1.073	1.197
Final R indexes [I≥2σ (I)]	R_1 = 0.0270, wR_2 = 0.0706	R_1 = 0.0660, wR_2 = 0.2133
Final R indexes [all data]	R_1 = 0.0289, wR_2 = 0.0723	R_1 = 0.0888, wR_2 = 0.2259
Largest diff. peak/hole (e.Å^{-3})	0.44/-0.59	0.90/-0.83
CCDC no	2521940	2443501

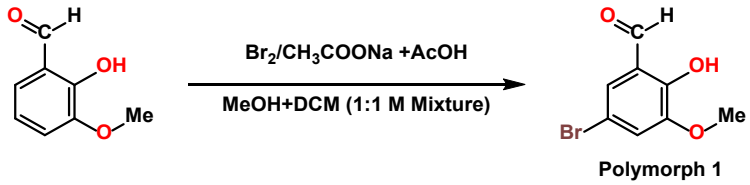

Scheme 1. Synthetic outline for polymorph 1.

The large and polarizable Br atom influences significant halogen-bonding interactions in crystal assembly, leading to the formation of various polymorphs [20-21]. These polymorphs also exhibit different colors and phosphorescent properties due to the presence of the Br atom and undergo a solid-solid transformation [22]. Furthermore, research on Br polymorphs has expanded to the stability of Br-containing drugs; for example, research on otilonium bromide identified a new stable polymorph [23]. Meanwhile, certain Br polymorphs, such as 2-Br-adamantane, are used in plastic crystal phases [24]. Today's research on Br polymorphs (8-bromotheophylline) focuses on multiple structural transformations [25]. Polymorphs are distinguished using various analytical techniques, including PXRD, DSC, FTIR, and Raman spectroscopic studies [26]. On the other hand, recent DFT research on Br polymorphs has attracted considerable attention from synthetic chemists working on polymorphs, as investigations have elucidated their reactivity, electronic structure, and unique supramolecular interactions [27]. Furthermore, research information was also obtained from integrated DFT studies based on FMO (HOMO-LUMO energy gap), global reactivity parameters, Hirshfeld surface/2D fingerprint plots, and calculations of interaction energy and energy frameworks.

This research article reports on one Br polymorph, its synthesis, structural characterization, X-ray crystal structure, and supramolecular interactions revealed in the crystal networks. In addition, significant supramolecular contacts were analyzed using the Hirshfeld surface and the 2D fingerprint plot. Finally, the interaction energy and energy frameworks were also calculated, revealing that the polymorph crystal frameworks are constructed from electrostatic (E_{ele}, red cylinders) and dispersion (E_{dis}, green cylinders) interactions. Furthermore, the article substantiates the polymorphic nature of compound 1 relative to the reported compound 2, using melting points, crystallographic insights, Hirshfeld surfaces, interaction energies, and energy frameworks.

2. Experimental

2.1. Materials and physical measurements

Analytical grade chemicals and solvents (CH_3OH and DCM) were used without further purification. Ortho-vanillin (CAS Number 148-53-8), CH_3COONa (CAS Number 127-09-3) and CH_3COOH (CAS Number 64-19-7) were purchased from Sigma-Aldrich. Polymorph elemental (%) was analyzed using a PerkinElmer 2400 CHN elemental instrument. HRMS analysis was analyzed using an Xevo G2-XS QToF 4K model. FT-IR (Infra-Red) spectra (4000-400 cm^{-1}) were collected using the PerkinElmer instrument. NMR spectra, including DEPT, were analyzed in $CDCl_3$ solvents with a Jeol JNM/ECZ 500R/S1 400 MHz NMR spectrometer. UV-VIS spectra were measured using a Hitachi U-3501 instrument over 200-800 nm at a solution concentration of 0.001 M.

2.2. Synthesis of polymorph 1

To synthesize a polymorph with high yield, we first purchased *ortho*-vanillin directly from Sigma-Aldrich. We followed the published literature methods [28,29], with slight modifications regarding the solvent medium. Scheme 1 outlines in detail the synthetic components and reaction medium, a mixed solvent of CH_3OH and DCM. Crystal growth of polymorph compounds was observed after slow evaporation from a mixed solvent medium at ambient temperature. The light-yellow needle-shaped single crystals suitable for SCXRD were immediately collected and air-dried in an open atmosphere.

(Polymorf 1) (Compound 2)

Figure 1. Perspective view of both forms.

5-Bromo-2-hydroxy-3-methoxybenzaldehyde (1): Color: Light yellow. Yield: 86%. M.p.: 125-129 °C for polymorph 1. M.p.: 120-121 °C for compound 2. FTIR (Solid, KBr, ν, cm^{-1}): 1580 ν(C=C), 2975 ν(O-CH_3), 1668 ν(C=O), 678 ν(C-Br). ^{1}H NMR (400 MHz, $CDCl_3$, δ, ppm):10.96 (s, 1H, OH), 9.81 (s, 1H, H-C=O), 7.25 (d, *J* = 2.2 Hz, 1H, Ar-H), 7.11 (d, *J* = 2.1 Hz, 1H, AR-H), 3.87 (s, 3H, CH_3). ^{13}C NMR (101 MHz, $CDCl_3$, δ ppm): 195.46 (s), 150.84 (s), 149.25 (s), 126.09 (s), 121.29 (s), 120.66 (s), 111.06 (s), 56.53 (s), ^{13}C DEPT NMR (126 MHz, $CDCl_3$, δ ppm): 120.47-131.87 (C Ar), 56.63-57.52, (O-CH_3), 190.85, (CHO). HRMS (EI, *m/z*) calcd. for $C_8H_7BrO_3$, 231.05; found 231.15. Anal. calcd. for $C_8H_7BrO_3$: C, 41.59; H, 3.05; Found: C, 41.63; H, 3.08%. UV/Vis (CH_3OH, λ_{max}, nm, (ε)):270 nm (ε = 1147 cm^{-1}) and 352 nm (ε = 728.7 cm^{-1}).

2.3. X-ray crystallography

For the polymorph, X-ray crystallographic data files were collected at room temperature (100 K). Table 1 summarizes all possible crystallographic data and structure refinement parameters used for crystal structure determination. A Bruker-AXS SMART APEX II diffractometer [30], equipped with standard Mo Kα radiation (λ = 0.71073 Å), was used. To solve the X-ray structure, programs including SMART, SAINT, and SADABS were used [31]. Notably, SHELXTL and least-squares programs were used to determine space group, structure, and F^2. Full-matrix least-squares methods refine the X-ray structure using SHELXL-2014 [32] and Olex-2 software [33-35]. Additionally, the X-ray structure was crystallo-graphically modified using anisotropic shift parameters for all atoms. The H-atoms were refined with isotropic parameters. Table 1 compares the polymorph 1 CIF data with a similar compound 2's reported CIF to better justify the formation of polymorph 1.

3. Results and discussion

3.1. Synthesis

The synthetic route is illustrated in Scheme 1. Polymorph 1 exhibits a higher melting point (>125 °C) than the previously reported analogous compound 2 (120-121 °C), while retaining good solubility in common organic solvents and excellent air stability. The newly obtained polymorph was comprehensively characterized using several analytical techniques, including HRMS and ^{1}H/^{13}C DEPT NMR spectroscopy. The authors previously reported compound 2 together with its crystal structure and antimicrobial properties [36]. However, the present crystal structure represents a distinct polymorphic form, as evidenced by differences in the crystallographic cell parameters (*a*, *b*, *c* and α, β, γ). The polymorphic nature is further supported by the CheckCIF analysis of the X-ray diffraction data, and a detailed comparison is provided in Table 1. Moreover, Hirshfeld surface analysis and the associated 2D fingerprint plots demonstrate notable differences in the intermolecular contact contributions between polymorph 1 and compound 2. In addition, interaction energy calculations and energy framework analyses further confirm the existence of a new polymorphic form. Notably, this study also presents, for the first time, a detailed investigation of the supramolecular noncovalent interactions governing the crystal packing network of polymorph 1.

3.2. Characterization

Several characterization techniques have been used for polymorph structural characterization purposes. These include HRMS, FT-IR, UV-VIS, and NMR spectroscopic studies. The Br polymorph is an aromatic compound, and its structural integrity is confirmed by HRMS in positive ion mode (Figure S2). The observed HRMS peaks were identified as *m/z* 231.15 $[M + H]^+$, while the calculated mass is 231.05. In addition, HRMS analysis ensures the stoichiometry and elemental composition of the polymorph. FTIR spectroscopy successfully confirms the presence of C-C, O-H, O-CH_3, C=O and C-Br stretching bands (cm^{-1}) in the polymorph. The observed significant FTIR peaks were ν(C=C), 1580, ν(O-CH_3), 2975, ν(C=O), 1668, and ν(C-Br), 678, respectively (Figure S1). The UV-vis spectra of the polymorph were recorded in MeOH (Figure S3). In this paper, the peaks observed at 270 and 352 nm are responsible for the π → π* electronic transition in an aromatic benzene ring. The polymorph is better structurally characterized by NMR spectroscopy (Figures S4-S6). The structural integrity is fully justified by NMR, including ^{1}H/^{13}C NMR. In polymorph 1, the ^{1}H NMR study confirms the proton nature, δ 7.11-7.25 (Ar-C*H*), 3.87 (O-CH_3), and 9.81 ppm (C*H*O), respectively. Similarly, the C-framework in polymorph 1 is supported by ^{13}C NMR peaks at δ 120.47-131.87 (CAr), 56.63-57.52 (O*C*H_3) and 190.85 ppm (*C*HO), respectively. Additionally, the structural polymorphic carbon framework is confirmed by ^{13}C DEPT decoupling NMR.

3.3. Crystal structure description

This article presents the X-ray crystal structures and supramolecular synthons of polymorph 1 and the previously reported 5-bromovanillin derivative 2. To clearly distinguish the structural differences between these two forms, a comparative analysis based on their X-ray diffraction data and crystallographic parameters was performed. Both compounds crystallize in the monoclinic crystal system with the space group $P2_1/c$; however, they exhibit distinct unit-cell parameters (*a*, *b*, *c*, α, β, and γ), confirming their polymorphic nature (Table 1). The molecular arrangements of both polymorphic forms are illustrated in Figure 1, while their structural overlay is presented in Figure 2. As shown in Figure 2, the free rotation of the aldehyde (-CHO) group gives rise to two distinct conformational arrangements. In form 2, a pronounced intramolecular hydrogen-bonding interaction is observed, which contributes significantly to its molecular conformation and crystal packing behaviour.

Table 2. Bond lengths for polymorph 1.

Atom 1	Atom 2	Length (Å)	Atom 3	Atom 4	Length (Å)
Br1	C4	1.901(3)	C5	C4	1.399(4)
O1	C1	1.218(3)	C6	C7	1.412(3)
O2	C7	1.347(3)	C3	C2	1.400(3)
O3	C6	1.364(3)	C3	C4	1.367(3)
O3	C8	1.427(3)	C7	C2	1.397(3)
C5	C6	1.373(4)	C2	C1	1.464(3)

Table 3. Bond angles for polymorph 1.

Atom 1	Atom 2	Atom 3	Angle (°)	Atom 4	Atom 5	Atom 6	Angle (°)
C6	O3	C8	117.8(2)	C2	C7	C6	119.4(2)
C6	C5	C4	119.8(2)	C3	C2	C1	120.1(2)
O3	C6	C5	125.8(2)	C7	C2	C3	120.4(2)
O3	C6	C7	114.2(2)	C7	C2	C1	119.5(2)
C5	C6	C7	120.0(2)	O1	C1	C2	124.2(2)
C4	C3	C2	118.8(2)	C5	C4	Br1	118.61(18)
O2	C7	C6	121.5(2)	C3	C4	Br1	119.30(19)
O2	C7	C2	119.1(2)	C3	C4	C5	122.1(2)

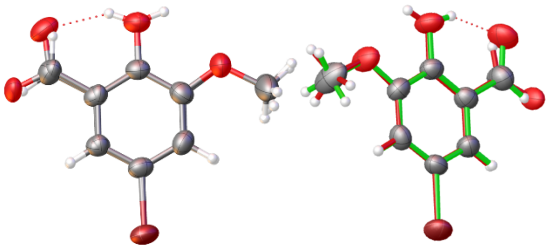

Figure 2. Perspective view of compound 2 forms.

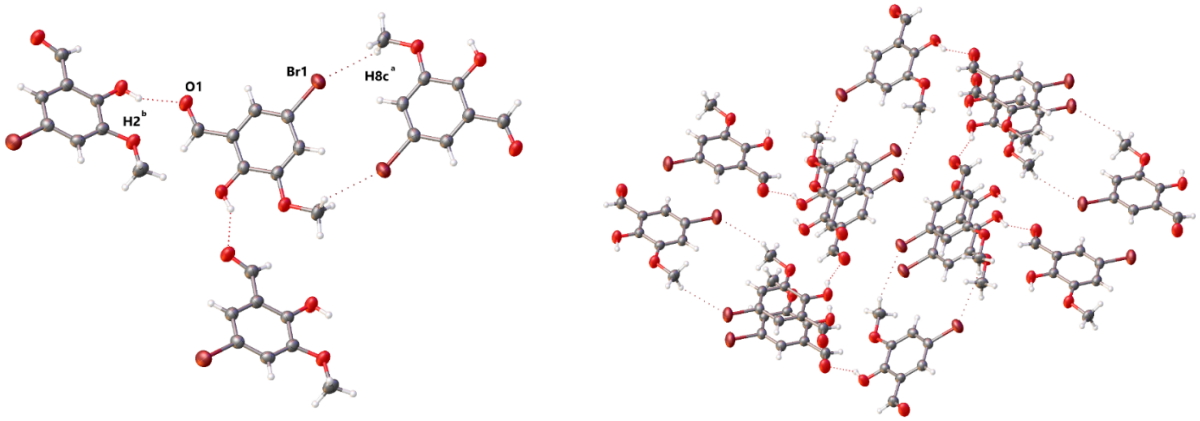

Figure 3. Perspective view hydrogen bonging interaction and crystal packing in polymorph 1 (a = 1-*x*, 1-*y*, 2-*z*, b = 1+*x*, 1/2-*y*, 1/2+*z*).

The complete crystallographic parameters for polymorph 1 are summarized in Tables 2 and 3, whereas the corresponding data for compound 2 are provided in Tables S1 and S2 in the Supplementary Information.

3.4. Supramolecular interactions

In polymorph 1 and compound 2, the supramolecular features are described in the following manner to ensure better structural integrity and polymorphic nature. In polymorph form 1, the bromine atom, Br(1), shows C-H···Br interaction with H(8C) (1-*x*, 1-*y*, 2-*z*). Another oxygen atom, O(1), forms a symmetry-related (1+*x*, 1/2-*y*, 1/2+*z*) O-H···O hydrogen bond with H(2) from the hydroxyl group. These interactions lead to the crystal packing shown in Figure 3. In contrast, in form 2 (reported), the bromine atom, Br(1), forms bifurcated hydrogen bonds. C-H···Br interaction with H(8C) (2-*x*, -1/2+*y*, 3/2-*z*) and weak O-H···Br contact with H(2) (*x*, -1+*y*, *z*). Another oxygen atom, O(1), forms an intramolecular O-H···O hydrogen bond with H(2) from the hydroxyl group. These interactions lead to the crystal packing shown in Figure 4. Therefore, the distinct supramolecular features confirm that polymorph 1 and compound 2 are different compounds. Furthermore, we have determined the melting point of 2, which is almost 120-121 °C. The determined melting point value differs by polymorph 1, confirming the polymorph formation from the synthetic perspective of Scheme 1. Polymorphs are distinct crystalline forms of the same molecule. Herein, generally, they exhibit different melting points due to variations in their internal lattice energy. This result has been reflected in polymorph 1 and reported in compound 2.

3.5. Hirshfeld surface and 2D fingerprint

In this section, we compared the Hirshfeld surface contacts for polymorph 1 and a similar reported compound 2. The Hirshfeld surface and 2D fingerprint analysis were conducted to reveal the NCI (noncovalent interactions) within the polymorph crystal framework [37].

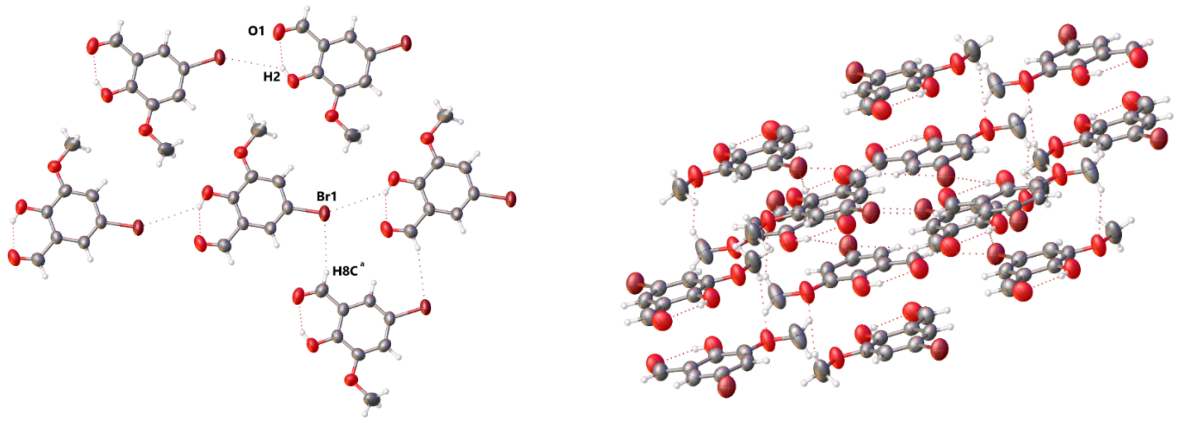

Figure 4. Perspective view hydrogen bonging interaction and crystal packing in compound 2 (a = 2-*x*, -1/2+*y*, 3/2-*z*, b = *x*, -1+*y*, *z*).

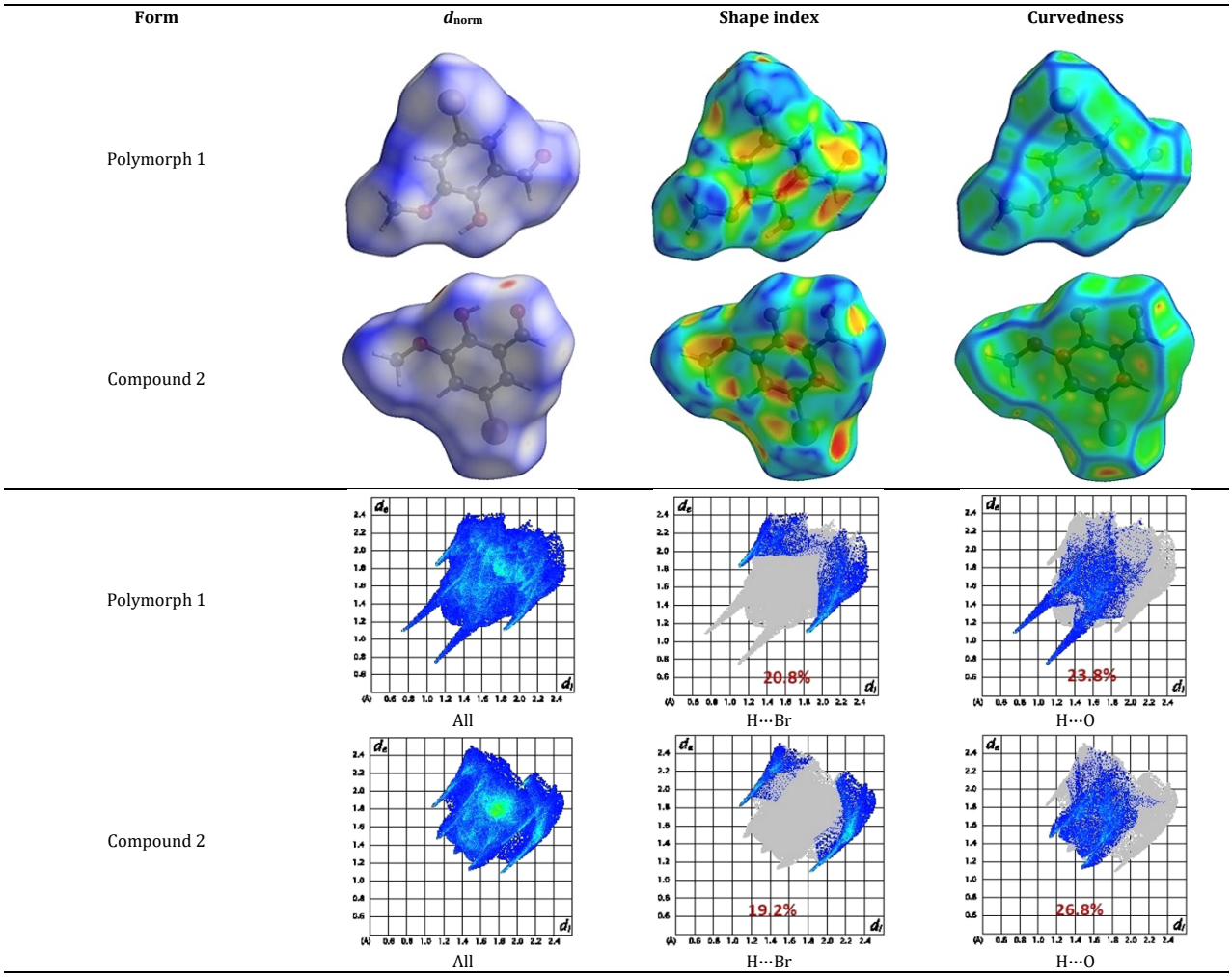

Figure 5. Hirshfeld surfaces mapped with d_{norm}, shape index, curvedness, and 2D fingerprint plot for the corresponding interactions for Polymorph 1 and compound 2.

The surfaces were mapped using d_{norm} (−0.5 to 1.5 Å), shape index (−1.0 to 1.0 Å), curvedness (−4.0 to 0.4 Å), and fragment patch (0 to 15 Å) (Figure 5). Different colored spots indicate different contacts. Notably, on the d_{norm} surfaces, deep blue and red circular regions correspond to shorter and longer intermolecular contacts, respectively, while white regions denote contacts at van der Waals radii. Prominent bright red areas highlight significant H···Br (20.8%) and H···O (23.8%) interactions. Furthermore, complementary 2D fingerprint plots (Figure 5) derived from d_e and d_i provide a quantitative representation of intermolecular contacts and interactions within the polymorph. Here, it is worth noting that reported similar contacts, 2 H···Br (19.2%) and H···O (26.8%), contribute differently to polymorph 1. The Hirshfeld surface contacts and 2D fingerprint calculations reveal that 1 is a polymorph.

Table 4. Different interaction energies of molecular pairs in kJ/mol for polymorph **1.**

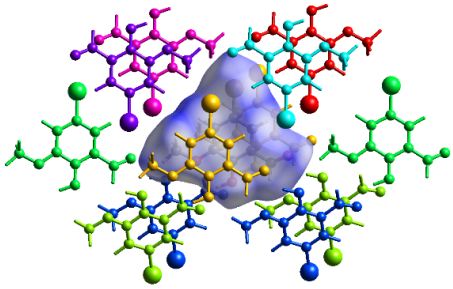

Color	N	Symmetry	R	E_{ele}	E_{pol}	E_{dis}	E_{rep}	E_{tot}
	1	-x, -y, -z	6.60	-8.3	-1.2	-13.9	10.0	-13.6
	1	x, y, z	4.08	2.0	-3.1	-46.2	22.2	-23.6
	0	x, -y+1/2, z+1/2	8.95	-37.6	-9.2	-16.0	35.3	-30.0
	1	x, y, z	10.11	-7.9	-1.7	-3.4	1.1	-11.4
	1	-x, -y, -z	5.52	-2.0	-0.5	-17.1	7.6	-11.6
	0	x, -y+1/2, z+1/2	8.31	4.7	-1.1	-12.6	3.3	-4.5
	0	-x, -y, -z	7.42	-2.7	-2.1	-12.2	6.2	-10.1
	1	-x, -y, -z	6.80	-6.9	-1.6	-13.1	9.2	-12.5

Table 5. Different interaction energies of molecular pairs in kJ/mol for compound 2.

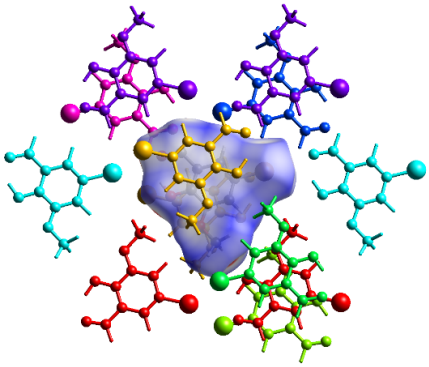

Color	N	Symmetry	R	E_{ele}	E_{pol}	E_{dis}	E_{rep}	E_{tot}
	2	-x, y+1/2, -z+1/2	8.28	-15.8	-5.0	-13.6	6.7	-26.2
	0	x, -y+1/2, z+1/2	4.09	-8.1	-3.2	-53.3	24.9	-38.2
	1	-x, -y, -z	8.72	1.5	-0.6	-3.3	0.1	-1.7
	1	-x, -y, -z	7.38	-0.3	-1.5	-10.5	2.4	-8.8
	1	x, y, z	9.42	-2.8	-0.4	-6.3	4.0	-5.5
	0	-x, -y, -z	6.76	-3.6	-0.7	-8.7	1.7	-10.6
	0	-x, y+1/2, -z+1/2	8.07	-10.3	-1.8	-9.6	7.9	-13.9
	0	-x, -y, -z	9.26	-12.2	-1.8	-9.3	6.8	-16.5

3.6. Interaction energy and energy frameworks

The interaction energy and energy frameworks were calculated by comparing polymorph 1 and compound 2 (Tables 4 and 5, and Figure 6). Intermolecular interaction energies were calculated using the HF/3-21G method available in Crystal Explorer 17. A molecular cluster was framed based on a crystallographic symmetry operation. It was a polymorph at a radius of 3.8 Å [37]. Herein, the total interaction energy (E_{tot}) = electrostatic (E_{ele}) + polarization (E_{pol}) + dispersion (E_{dis}) + exchange-repulsion (E_{rep}) components. To do this, the scale factors were 1.019, 0.651, 0.901, and 0.811 [38]. The calculated energies (kJ/mol) are: –58.7 (E_{ele}), –20.5 (E_{pol}), –134.5 (E_{dis}), 94.9 (E_{rep}) and –117.3 (E_{tot}) for polymorph 1; and –51.6 (E_{ele}), –15.0 (E_{pol}), –114.6 (E_{dis}), 54.5 (E_{rep}), and –121.4 (E_{tot}) for compound 2. Furthermore, energy frameworks provide a visual representation of intermolecular interaction energies and their relative magnitudes [39]. In these frameworks, molecular pair interactions are depicted as cylinders connecting molecular centroids, with the radius of the cylinder proportional to the corresponding energy [40]. For polymorph 1 and compound 2, the constructed frameworks revealed electrostatic (E_{ele}, red cylinders), dispersion (E_{dis}, green cylinders), and total interaction energies (E_{tot}, blue cylinders) (Figure 6). Therefore, the interaction energy and energy framework calculations for polymorph 1 and compound 2 yield different coulombic, dispersion, and total energy results. Consequently, polymorph 1 is polymorphic and different from the reported similar compound 2.

4. Conclusions

We report the synthesis, characterization, crystal structure, and noncovalent supramolecular interactions of polymorph 1, a newly synthesized polymorph, highlighting the importance of polymorphism in chemistry. Polymorph 1 was structurally characterized by FTIR, HRMS, UV-VIS, $^{1}H/^{13}C$-NMR, and ^{13}C DEPT NMR spectroscopy. The polymorphic nature of polymorph 1 over compound 2 is investigated by different research perspectives, including melting point, Hirshfeld surface contacts, supramolecular features, and finally interaction energies and energy frameworks (coulombic, dispersion, and total energy values). The X-ray structure reveals that polymorph 1 crystalizes in the monoclinic space group $P2_1/c$, with distinct *a*, *b*, *c*, α, β, and γ cell parameters.

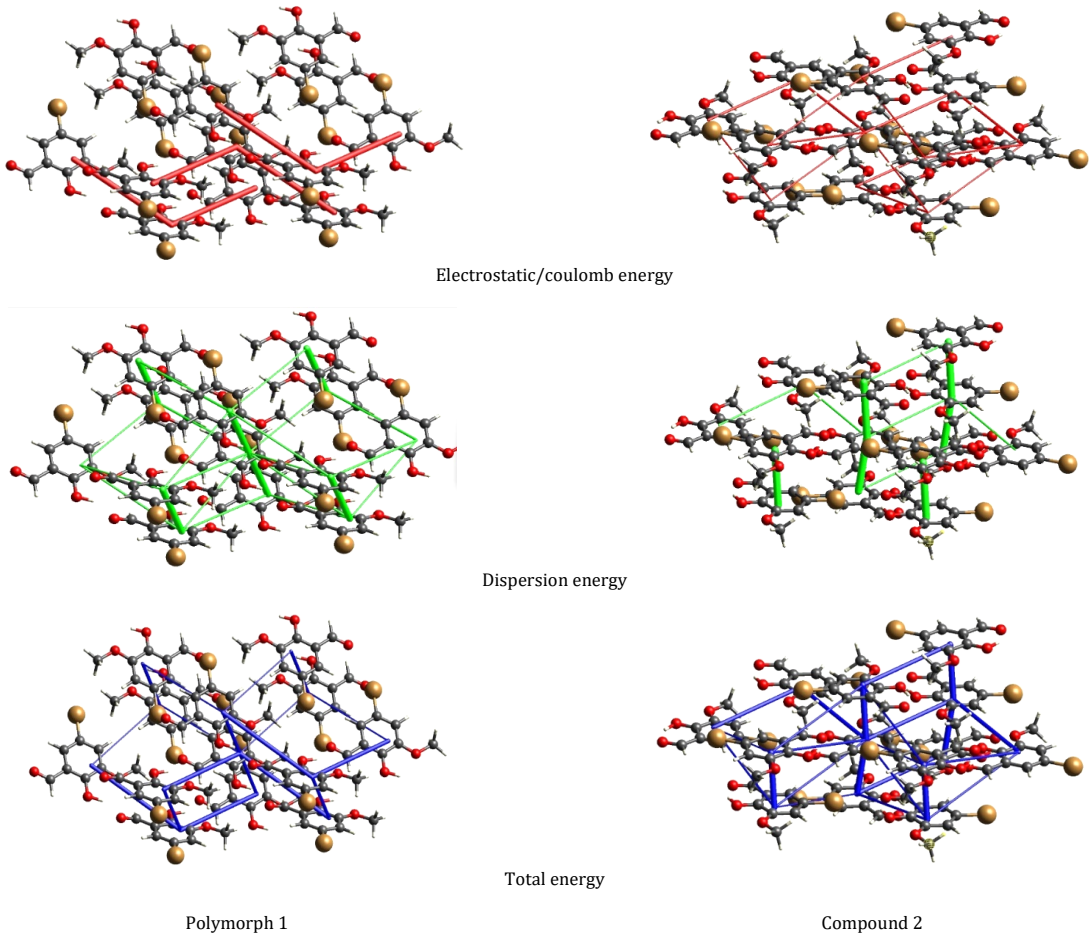

Figure 6. Perspective views of electrostatic/coulomb energy, dispersion energy, total energy diagrams, for a cluster of molecules in polymorph 1 and compound 2. The cylindrical radius is proportional to the relative strength of the corresponding energies. The scale factor used is 50 with cut-off values of 10 kJ/mol.

The only significant supramolecular interactions observed in the crystal networks are C-H···Br and O-H···O hydrogen bonds. Furthermore, Hirshfeld surface and 2D fingerprint plots identify significant H···Br (20.8%) and H···O (23.8%) in the crystal assembly. In polymorph 1, molecular interaction energies and energy frameworks reveal that constructed frameworks belong to the electrostatic (E_{ele}) and dispersion (E_{dis}) categories, in addition to the total interaction energies (E_{tot}).

Acknowledgements

The authors acknowledge the Central Laboratory of Tamralipta Mahavidyalaya and the Department of Chemistry, Tamluk-721636, Purba Medinipur, WB, India. The authors are also thankful to Indian Institute of Technology (IIT) Jammu, Saptarshi Laboratory, Paloura campus, India, for providing advanced characterization data files, including HRMS and $^{1}H/^{13}C$-DEPT decoupling NMR and for FTIR and UV-vis analysis, the Department of Chemistry and Chemical Technology, Vidyasagar University, Midnapore-721102, West Bengal, India.

Supporting information

CCDC 2521940 (Polymorph 1) and 2443501 (Compound 2) contain the supplementary crystallographic data for this paper. These data can be obtained free of charge via www.ccdc.cam.ac.uk/data_request/cif, or by e-mailing data_request@ccdc.cam.ac.uk, or by contacting The Cambridge Crystallographic Data Centre, 12 Union Road, Cambridge CB2 1EZ, UK; fax: +44(0)1223-336033. The Electronic Supplementary Information (ESI) includes the bond lengths and bond angles of the previously reported compound 2, together with the FT-IR and HRMS spectra of polymorph 1, as well as the UV-Vis, ^{1}H NMR, ^{13}C NMR, and ^{13}C DEPT NMR.

Disclosure statement

Conflict of interests: The authors declare that they have no conflict of interest.
Ethical approval: All ethical guidelines have been adhered to.
Data availability: All experimental data are available upon reasonable request from the author.

CRediT authorship contribution statement

Conceptualization: Dhrubajyoti Majumdar, Sourav Roy; Methodology: Dhrubajyoti Majumdar; Software: Dhrubajyoti Majumdar, Sourav Roy, Dhiraj Das; Validation: Dhrubajyoti Majumdar, Sourav Roy; Formal Analysis: Dhrubajyoti Majumdar, Sourav Roy, Dhiraj Das; Investigation: Dhrubajyoti Majumdar; Resources: Dhrubajyoti Majumdar; Data Curation: Dhrubajyoti Majumdar, Sourav Roy; Writing - Original Draft: Dhrubajyoti Majumdar, Sourav Roy; Writing - Review and Editing: Dhrubajyoti Majumdar, Sourav Roy; Visualization: Dhrubajyoti Majumdar, Sourav Roy, Dhiraj Das; Supervision: Dhrubajyoti Majumdar; Project Administration: Dhrubajyoti Majumdar.

ORCID and Email

Sourav Roy
souravscott@gmail.com
https://orcid.org/0000-0002-3919-7715
Dhrubajyoti Majumdar
dmajumdar30@gmail.com
https://orcid.org/0000-0002-9785-7750
Dhiraj Das
dhirajdasiitkjp@gmail.com
https://orcid.org/0000-0003-2646-7226

References

[1]. Chen, A.; Peng, Y.; Chen, Z.; Lu, Y.; Guo, M.; Cai, T. Crystal engineering for poorly water-soluble drugs: From design to applications. *Acta Pharm. Sin. B* **2026**, *16* (4), 1848–1882.

[2]. Rissanen, K. Crystallography and Crystal Engineering. *Anal. Methods Supramol. Chem.* **2012**, 459–498.

[3]. Nangia, A. K.; Desiraju, G. R. Crystal Engineering: An Outlook for the Future. *Angew. Chem. Int. Ed.* **2019**, *58* (13), 4100–4107.

[4]. Higashi, K.; Ueda, K.; Moribe, K. Recent progress of structural study of polymorphic pharmaceutical drugs. *Adv. Drug Deliv. Rev.* **2017**, *117*, 71–85.

[5]. Aitipamula, S.; Banerjee, R.; Bansal, A. K.; Biradha, K.; Cheney, M. L.; Choudhury, A. R.; Desiraju, G. R.; Dikundwar, A. G.; Dubey, R.; Duggirala, N.; Ghogale, P. P.; Ghosh, S.; Goswami, P. K.; Goud, N. R.; Jetti, R. R.; Karpinski, P.; Kaushik, P.; Kumar, D.; Kumar, V.; Moulton, B.; Mukherjee, A.; Mukherjee, G.; Myerson, A. S.; Puri, V.; Ramanan, A.; Rajamannar, T.; Reddy, C. M.; Rodriguez-Hornedo, N.; Rogers, R. D.; Row, T. N.; Sanphui, P.; Shan, N.; Shete, G.; Singh, A.; Sun, C. C.; Swift, J. A.; Thaimattam, R.; Thakur, T. S.; Kumar Thaper, R.; Thomas, S. P.; Tothadi, S.; Vangala, V. R.; Variankaval, N.; Vishweshwar, P.; Weyna, D. R.; Zaworotko, M. J. Polymorphs, Salts, and Cocrystals: What's in a Name?. *Cryst. Growth Des.* **2012**, *12* (5), 2147–2152.

[6]. Vippagunta, S. R.; Brittain, H. G.; Grant, D. J. Crystalline solids. *Adv. Drug Deliv. Rev.* **2001**, *48* (1), 3–26.

[7]. Gao, L.; Dai, X.; Li, S.; Vasilev, N. A.; Perlovich, G. L.; Lu, T.; Chen, J. Effect of Polyamorphism on the Morphology, Dissolution, and Stability of Olaparib. *Cryst. Growth Des.* **2024**, *24* (12), 4906–4913.

[8]. Gao, Z.; Rohani, S.; Gong, J.; Wang, J. Recent Developments in the Crystallization Process: Toward the Pharmaceutical Industry. *Engineering* **2017**, *3* (3), 343–353.

[9]. Kitamura, M. Strategy for control of crystallization of polymorphs. *CrystEngComm* **2009**, *11* (6), 949–964.

[10]. Brittain, H. G. Polymorphism in Pharmaceutical Solids, Second Edition; Informa Medical, 2009.

[11]. Censi, R.; Di Martino, P. Polymorph Impact on the Bioavailability and Stability of Poorly Soluble Drugs. *Molecules* **2015**, *20* (10), 18759–18776.

[12]. Nicoud, L.; Licordari, F.; Myerson, A. S. Estimation of the Solubility of Metastable Polymorphs: A Critical Review. *Cryst. Growth Des.* **2018**, *18* (11), 7228–7237.

[13]. Agostini, S. B.; Borges, B. A.; de Araújo, M. B.; Bonfilio, R. Growing Interest in Pharmaceutical Cocrystals: A Comprehensive Review of Applications and Trends. *ChemistrySelect* **2025**, *10* (30) e00831, https://doi.org/10.1002/slct.202500831.

[14]. Malik, A. A.; Gupta, P.; Joseph, A. Crystal polymorphism: Applications and future prospects. *AIP Conf. Proc.* **2023**, *2804*, 020039.

[15]. Feng, Y.; Hao, H.; Chen, Y.; Wang, N.; Wang, T.; Huang, X. Enhancement of Crystallization Process of the Organic Pharmaceutical Molecules through High Pressure. *Crystals* **2022**, *12* (3), 432.

[16]. Saha, B. K.; Nath, N. K.; Thakuria, R. Polymorphs with Remarkably Distinct Physical and/or Chemical Properties. *Chem. Rec.* **2022**, *23* (1), e202200173 https://doi.org/10.1002/tcr.202200173.

[17]. Parrish, D. A.; Deschamps, J. R.; Gilardi, R. D.; Butcher, R. J. Polymorphs of Picryl Bromide. *Cryst. Growth Des.* **2007**, *8* (1), 57–62.

[18]. Gowrisankar, S.; Fokin, A. A.; Becker, J.; Mathew, N.; Schmedt auf der Günne, J.; Schreiner, P. R. Polymorphism and White Light Emission of 1-Bromo-3,5,7-triphenyladamantane Compared with 1,3,5,7-Tetraphenyladamantane. *Eur J. Org Chem* **2024**, *27* (23), e202400260 https://doi.org/10.1002/ejoc.202400260.

[19]. Krishnapriya, B.; Malarselvi, R.; Raja, C.; Priscilla, R. Elucidation of crystal structures using Bragg's peaks and Nuclear Magnetic Resonance chemical shifts for polymorphic forms of (E)-4-Bromo-2-[(phenylimino)methyl]phenol. *Chem. Phys. Impact* **2023**, *7*, 100340.

[20]. Gilday, L. C.; Robinson, S. W.; Barendt, T. A.; Langton, M. J.; Mullaney, B. R.; Beer, P. D. Halogen Bonding in Supramolecular Chemistry. *Chem. Rev.* **2015**, *115* (15), 7118–7195.

[21]. Usoltsev, A. N.; Sukhikh, T. S.; Novikov, A. S.; Shayapov, V. R.; Pishchur, D. P.; Korolkov, I. V.; Sakhapov, I. F.; Fedin, V. P.; Sokolov, M. N.; Adonin, S. A. Unexpected Polymorphism in Bromoantimonate(III) Complexes and Its Effect on Optical Properties. *Inorg. Chem.* **2021**, *60* (4), 2797–2804.

[22]. Gavale, R.; Pandit, S. K.; Misra, R. Room Temperature Phosphorescence Driven by Mechanochromism. *Chem. An Asian J.* **2025**, *20* (10), e202401893 https://doi.org/10.1002/asia.202401893.

[23]. Vega, D. R.; Halac, E.; Segovia, L.; Baggio, R. A New, More Stable Polymorphic Form of Otilonium Bromide: Solubility, Crystal Structure, and Phase Transformation. *J. Pharm. Sci.* **2016**, *105* (10), 3013–3020.

[24]. Negrier, P.; Barrio, M.; Tamarit, J. L.; Mondieig, D. Polymorphism in 2-X-Adamantane Derivatives (X = Cl, Br). *J. Phys. Chem. B.* **2014**, *118* (32), 9595–9603.

[25]. Ye, W.; Zhang, C.; Sung, H. H.; Wong, L. W.; Sheong, F. K.; Williams, I. D. Effect of Molecular Perturbation on Polymorphism: The Case of 8-Halotheophyllines (8-Cl-Tph and 8-Br-Tph). *Crystals* **2025**, *15* (4), 340.

[26]. Kuang, Y.; Gao, X.; Niu, Y.; Shi, X.; Zhou, W. Polymorphic Characterization, Pharmacokinetics, and Anti-Inflammatory Activity of Ginsenoside Compound K Polymorphs. *Molecules* **2021**, *26* (7), 1983.

[27]. Berezin, A. Non-centrosymmetric triclinic polymorph of bis(triphenylphosphine oxide)copper(II) dibromide: Crystal structure, magnetic properties, and DFT calculations. *J. Mol. Struct.* **2026**, *1353*, 144733.

[28]. Wang, L. P.; Liu, D. W.; Wang, G. P.; Qin, S. L.; Huang, S. P.; Wang, X. J. Study on Synthesis of 6-Bromo-2, 3-Dihydroxybenzaldehyde. *Adv. Mat. Res.* **2014**, *1033-1034*, 552–554.

[29]. Hanson, J. R.; Hitchcock, P. B.; Toche, F. The Conformation of Some *ortho*-bromoarylaldehydes. *J. Chem. Res.* **2008**, *2008* (7), 416–418.

[30]. Chakraborty, J.; Thakurta, S.; Samanta, B.; Ray, A.; Pilet, G.; Batten, S. R.; Jensen, P.; Mitra, S. Synthesis, characterisation and crystal structures of three trinuclear cadmium(II) complexes with multidentate Schiff base ligands. *Polyhedron* **2007**, *26* (17), 5139–5149.

[31]. Bruker (2008). SMART, SAINT. Bruker AXS Inc., Madison, Wisconsin, USA.

[32]. Sheldrick, G. M. Crystal Structure Refinement with SHELXL. *Acta Crystallogr. C Struct. Chem.* **2015**, *71* , 3–8.

[33]. Dolomanov, O. V.; Bourhis, L. J.; Gildea, R. J.; Howard, J. A.; Puschmann, H. *OLEX2*: a complete structure solution, refinement and analysis program. *J. Appl. Crystallogr.* **2009**, *42* (2), 339–341.

[34]. Sheldrick, G. M. A short history of *SHELX*. *Acta Crystallogr. A. Found Crystallogr.* **2007**, *64* (1), 112–122.

[35]. Sheldrick, G. M. SHELXTL: Software for Empirical Absorption Correction, Version 6.12; Bruker AXS Inc.: Madison, WI, 2001.

[36]. Majumdar, D.; Das, D.; Philip, J. E.; Tuzun, B.; Roy, S. Synthesis, Crystal Engineering, Density Functional Theory, ADME/T, Molecular Docking, and Antimicrobial Evaluation of Bromo-Based Ortho-Vanillin Compounds. *ChemistrySelect* **2025**, *10* (35), e02364 https://doi.org/10.1002/slct.202502364.

[37]. Turner, M. J.; Grabowsky, S.; Jayatilaka, D.; Spackman, M. A. Accurate and Efficient Model Energies for Exploring Intermolecular Interactions in Molecular Crystals. *J. Phys. Chem. Lett.* **2014**, *5* (24), 4249–4255.

[38]. Venkatesan, P.; Thamotharan, S.; Ilangovan, A.; Liang, H.; Sundius, T. Crystal structure, Hirshfeld surfaces and DFT computation of NLO active (2E)-2-(ethoxycarbonyl)-3-[(1-methoxy-1-oxo-3-phenylpropan-2-yl)amino] prop-2-enoic acid. *Spectrochim. Acta A: Mol. Biomol. Spectrosc.* **2016**, *153*, 625–636.

[39]. Turner, M. J.; Thomas, S. P.; Shi, M. W.; Jayatilaka, D.; Spackman, M. A. Energy frameworks: insights into interaction anisotropy and the mechanical properties of molecular crystals. *Chem. Commun.* **2015**, *51* (18), 3735–3738.

[40]. Yuan, G.; Shao, K.; Du, D.; Wang, X.; Su, Z.; Ma, J. Secondary ligand-directed assembly of metal–organic coordination polymers based on a 2-(pyridin-4-yl)-1H-imidazole-4,5-dicarboxylic acid ligand: Syntheses, structures and photoluminescent properties. *CrystEngComm.* **2012**, *14* (5), 1865–1873.